Submitted, accepted and published by:
Chemical Engineering Journal 405 (2021) 126679
https://doi.org/10.1016/j.cej.2020.126679

Biomass Chemical Looping Gasification for syngas production using ilmenite as oxygen carrier in a 1.5 kW_{th} unit

Oscar Condori, Francisco García-Labiano*, Luis F. de Diego, María T. Izquierdo, Alberto Abad, Juan Adánez

Instituto de Carboquímica (ICB-CSIC). Miguel Luesma Castán 4, 50018 Zaragoza, Spain

*E-mail: glabiano@icb.csic.es

Abstract

Biomass Chemical Looping Gasification, BCLG, is a promising technology that uses lattice oxygen instead of expensive gaseous oxygen for high quality syngas production without CO_2 emissions. In this work, 55 hours of continuous operation in a 1.5 kW_{th} BCLG unit using ilmenite as oxygen carrier and pine wood as fuel is reported. A new method for controlling the oxygen used in the syngas production through the control of the oxygen fed into the air reactor was used by first time in BCLG with satisfactory results. This method allows analysing the isolated effect of each one of the operating conditions: gasification temperature, T_{FR}, steam-to-biomass ratio, S/B, and oxygen-to-biomass ratio, λ. This last parameter, λ, was the main factor affecting syngas production efficiency. Considering the high unconverted hydrocarbons usually obtained, a product gas composed by 37-40 % CO_2; 27-30% H_2; 17-21% CO; 10-12% CH_4; and 2-3% C2-C3 with a syngas yield of 0.65 Nm^3/kg dry biomass could be obtained at autothermal conditions. Tar generation was in the range 1.4-3.0 g/kg dry biomass (1-2.5 g/Nm^3 d.b.), being lower than that reported by other gasification technologies. Despite its high reduction state in BCLG, ilmenite exhibited a good behaviour since remained with high reactivity during operation and no agglomeration problems were produced.

Submitted, accepted and published by:
Chemical Engineering Journal 405 (2021) 126679
https://doi.org/10.1016/j.cej.2020.126679

However, outward migration of Fe observed in ilmenite decreased lifetime by a half during CLG operation in relation to chemical looping combustion conditions.

Keywords: biomass; syngas; chemical-looping gasification; ilmenite; tars

1. Introduction

The use of liquid biofuels on the transport sector has been identified as one of the most relevant alternatives to reduce CO_2 emissions to the atmosphere, as implemented by the Paris Agreement on Climate Change. The use of a renewable source as biomass in a gasification process would allow the production of a synthesis gas that may be used for liquid fuels production via Fisher Tropsch (FT) synthesis [1]. There are different commercial available technologies for gasification [2]. However, Biomass Chemical Looping Gasification (BCLG) represents an innovative process with the potential of reducing costs and emissions compared to other gasification technologies [3-6]. In BCLG, a solid oxygen carrier circulates between two interconnected fluidized bed reactors, fuel and air reactors, providing the oxygen needed for partial oxidation of the solid fuel and the heat necessary for the endothermic reactions taking place for syngas production. The main advantage of BCLG is the production of high quality syngas, non-diluted in nitrogen, without using costly pure oxygen and without CO_2 emissions to the atmosphere. In fact, BCLG process can operate at autothermal conditions with all the carbon compounds exiting the system in the fuel reactor stream. The separation and further storage of the CO_2 present in the syngas allows CLG operation without any emission.

The schematic illustration of this process is shown in Figure 1. The biomass is converted into gaseous (pyrolysis gas), liquid (tar) and solid (char) products in the fuel reactor and then these products may be partially oxidized by the oxygen carrier and the gasifying agent. Thus, solid fuel is converted to synthesis gas and the oxygen carrier is reduced in parallel. The oxygen carrier is denoted by Me_xO_y and Me_xO_{y-1}, where Me_xO_y is a metal oxide and Me_xO_{y-1} its reduced compound.

Submitted, accepted and published by:
Chemical Engineering Journal 405 (2021) 126679
https://doi.org/10.1016/j.cej.2020.126679

The reduced oxygen carrier goes to the air reactor where it is regenerated in air atmosphere to begin a new cycle. Moreover, the reactions that occur in the air reactor are exothermic, so the required heat for fuel gasification is provided by the circulating oxygen carrier from the air to the fuel reactor.

A key aspect in the development of the BCLG process is the selection of a suitable oxygen carrier. The solid oxygen carrier should have the capability to transport oxygen that is included in the crystal lattice. Many metal oxides based on Fe, Cu, Ni, and Mn have been used as oxygen carriers. Currently there is wide experience on the behaviour of these materials in Chemical Looping Combustion (CLC) processes [7-8]. However, the conditions existing in the fuel reactor in BCLG are quite different to CLC, expecting an oxygen carrier working at more reduced conditions. In this sense, much lower experience exists about the behaviour of oxygen carriers under CLG conditions. Oxygen carriers based on Ni, Cu, Mn and even perovskites have been proposed for BCLG although majority are based on Fe due to the competitive prices and environmental compatibility. To improve properties regarding their use in BCLG, synthetic materials have been manufactured including both pure Fe_2O_3 [9-12] or supported on an inert high-temperature material which can significantly increase the reactivity, durability, and lifetime of oxygen carrier. The use of bimetallic compounds such as Fe-Ni [13-16], Fe-Ni-Al [17], Fe-Cu [18-20], Fe-Ca [21-23] and Fe-Ba-Al [24] has been also studied. In this sense, although synthetic materials could significantly improve the properties of the oxygen carriers, the use of low-cost natural iron ores represents an attractive material for BGCL because of its abundance and low price.

Although laboratory batch fluidized bed reactors and thermogravimetric analysers (TGA) can be useful in the first steps of development to know the suitability of an oxygen carrier, its performance under continuous operation is necessary. However, limited number of studies related to BCLG technology in continuous operation units can be found in literature including both synthetic and natural materials. Virginie et al. [25] used olivine impregnated with iron during the operation under indirect gasification process in a 1.5 kW_{th} dual fluidized bed. They found a positive effect on the

Submitted, accepted and published by:
Chemical Engineering Journal 405 (2021) 126679
https://doi.org/10.1016/j.cej.2020.126679

incorporation of an oxygen carrier in the bed through a reduction in tar generation. Wei et al. [5] and Huseyin et al. [26] assessed the behaviour of a synthetic Fe_3O_4/Al_2O_3 oxygen carrier in a 10 kW_{th} CLG unit. They reported 20 h of continuous operation using sawdust pine as fuel to analyse different operating conditions including temperature and biomass feeding rate. To operate under gasification conditions they used a constant solid circulation rate and increasing biomass feeding rate. Later, Wei et al. [16] used Fe-Ni bimetallic oxygen carriers in the same 10 kW_{th} unit to improve reactivity and therefore the gasification efficiency. Ge et al. [6, 27] evaluated the behaviour of two different oxygen carriers, a synthetic NiO/Al_2O_3 and a natural hematite, in a 25 kW_{th} CLG unit. The authors diluted the oxygen carrier with silica sand to maintain constant the fuel reactor temperature and to decrease the amount of lattice oxygen in the process. Finally, Shen et al. [28] investigated the CLG performance of coal in a 5 kW_{th} unit using as oxygen carrier natural hematite alone or blended with silica sand to improve fluidization. They used a two-stage-based circulating bed as fuel reactor to increase gasification performance and reduce CH_4 content. The above works carried out in continuous units used different methods to control the oxygen to fuel ratios. However, these methods did not allow the study of the isolated effect of each operating condition since they were usually linked among them or produced variations in the fluid-dynamic properties of the system.

Regarding oxygen carrier selection, most of the materials used in BCLG have been previously used for CLC [7,8]. One of the most promising low cost materials widely used in CLC is ilmenite, $FeTiO_3$. This material has been tested in CLC continuous units at scales of 0.5 and 50 kW at ICB-CSIC [29-30], 10 and 100 kW at CUT [31-32], 25 kW at TUHH [33], and 1 MW at TUD [34]. Ilmenite has been also used in the called Oxygen Carrier aided Combustion (OCAC) process, where long tests at high scale, 12 MW [35] and 75MW_{th} [36], have been carried out using biomass and municipal solid waste as fuel. However, ilmenite has never been tested in BCLG conditions.

The objective of this work was to study by first time the behaviour of ilmenite as oxygen carrier in a 1.5 kW_{th} BCLG continuous unit to obtain a highly concentrated synthesis gas stream using wood

Submitted, accepted and published by:
Chemical Engineering Journal 405 (2021) 126679
https://doi.org/10.1016/j.cej.2020.126679

pine as fuel. The work included the analysis of the isolated effect of each one of the operating condition. Thus, the fuel reactor temperature, steam-to-biomass ratio, or oxygen-to-biomass ratio were varied while the rest of the operating conditions were kept constant. This was possible through the use of a new method for controlling the lattice oxygen used for syngas production that allow maintaining constant the fluid-dynamic properties of the system when using different operating conditions. Ilmenite was selected as oxygen carrier considering the good results obtained previously in other related chemical looping processes such as in-situ gasification CLC (*iG*-CLC) or OCAC. A complete characterization of the ilmenite along the operation time in CLG was carried out and compared to its behaviour at combustion conditions. Finally, a dedicated analysis with respect to tar production at different operating conditions was performed in order to experimentally demonstrate the benefits of BCLG in comparison with other gasification processes.

2. Experimental.

2.1. Materials.

Ilmenite provided by the Norwegian company Titania A/S was used as oxygen carrier. Ilmenite is extracted from a natural ore mainly composed by iron titanium oxide and it was received in its reduced form $FeTiO_3$. Fresh ilmenite particles underwent a first treatment consisting of calcination at 950ºC in an air atmosphere for 24 hours to improve the physical properties and initial reaction rates and to avoid defluidization problems [29]. Table 1 shows the main properties for the calcined ilmenite that were determined by using several characterization techniques such as Hg porosimetry, helium pycnometry, thermogravimetric analysis, etc. A Bruker D8 Advance polycrystalline powder X-ray diffractometer (XRD) was used to carry out qualitative and quantitative analyses of crystalline phases that integrate the oxygen carrier in its reduced and oxidized forms. The XRD analysis of the calcined ilmenite showed that it was mainly composed by Fe_2TiO_5 (pseudobrookite) and TiO_2 (rutile), with lower amount of Fe_2O_3 (hematite). The composition of calcined ilmenite was 54.7 wt% Fe_2TiO_5, 11.2 wt% Fe_2O_3, 28.6 wt% TiO_2 and 5.5 wt% of other inert compounds. The surface

Submitted, accepted and published by:
Chemical Engineering Journal 405 (2021) 126679
https://doi.org/10.1016/j.cej.2020.126679

morphology and characteristics of the samples were analysed in an SEM-EDX Hitachi S-3400 N with the EDX Röntec XFlash of Si (Li) analyser. Furthermore, it was possible to observe the dispersion of the different compounds (Fe, Ti, O) throughout a cut of the particle.

The oxygen transport capacity for the calcined ilmenite ($R_{O,ilm}$), defined as the mass fraction of the oxygen-carrier that is used for oxygen transfer, was determined in a thermobalance (CI Electronics). A value of 4.03 wt% was obtained that corresponds to the oxygen transferred by the redox pairs Fe_2TiO_5/ $FeTiO_3$ and Fe_2O_3 / Fe_3O_4. The particle size of the oxygen carrier used during the process was 100-300 μm.

Pine wood biomass from pellets supplied by TU Darmstadt (Germany) was used as renewable solid fuel. The biomass pellets were milled and sieved to obtain a particle size in the range 0.5-2 mm. Table 2 shows the proximate and ultimate analysis of the biomass.

2.2. BCLG reactions with ilmenite

The reactions that occur during the BCLG process when using ilmenite as oxygen carrier are shown below. The difference with the *iG*-CLC process is that the amount of lattice oxygen used in BCLG is lower. In fact, biomass is devolatilized when it is introduced into the fuel reactor producing gases, tar and char, (R1). Then, the carbon present in char is gasified with steam, (R2), or CO_2, (R3), to give syngas. The presence of oxygen carrier inside the fuel reactor introduces new possible reactions. Both the Fe_2TiO_5 and the Fe_2O_3 can react with the gases generated during biomass devolatilization and char gasification to produce CO_2 and H_2O, (R4)-(R6) and (R8)-(R10). Some other gas-gas reactions include the partial oxidation of CH_4 or light hydrocarbons (R7)-(R11), the methane (light hydrocarbons) reforming with steam and CO_2 (R12)-(R13) or the water gas shift (R14), which can be catalysed by the iron compounds present in the bed. Some potential reactions of tars have been reported in the literature [26, 37-38], the most relevant being tar cracking into smaller molecular weight gases (R15), tar reforming catalysed by iron (R16), and even tar combustion with the oxygen carrier (R17)-(R18).

Submitted, accepted and published by:
Chemical Engineering Journal 405 (2021) 126679
https://doi.org/10.1016/j.cej.2020.126679

(R1)

(R2)

(R3)

(R4)

(R5)

(R6)

(R7)

(R8)

(R9)

(R10)

(R11)

(R12)

CH_4 (C_xH_y) + CO_2 → 2CO + $2H_2$ (R13)

(R14)

(R15)

(R16)

(R17)

Tar + $3Fe_2O_3$→ $2Fe_3O_4$ + CO_2 + H_2O (R18)

The reduced oxygen carrier is sent to the air reactor to be regenerated with air, (R19)-(R20). Some char can also reach the air reactor where it is burnt to give CO_2, (R21), which produces a decrease in the carbon conversion efficiency in the process and produces CO_2 emissions to the atmosphere. These reactions are always exothermic and are the responsible for heat generation that will be transported to the fuel reactor for the endothermic gasification reactions.

(R19)

Submitted, accepted and published by:
Chemical Engineering Journal 405 (2021) 126679
https://doi.org/10.1016/j.cej.2020.126679

(R20)

(R21)

2.4. Chemical Looping Gasification unit at ICB-CSIC.

Figure 2 shows a diagram of the 1.5 kW_{th} chemical looping unit located at ICB-CSIC used in this work for BCLG. This unit has been previously used for coal and biomass *iG*-CLC using ilmenite as oxygen carrier [29] and for indirect gasification processes using a Fe-olivine material [25]. The unit consists of two bubbling interconnected fluidized beds, fuel (FR) and air (AR) reactors, with solids circulating between them. Two loop seals avoid gas mixing between both reactors. Several furnaces installed in the unit are used to better control the temperature inside the reactors. The biomass is fed to the fuel reactor by means of two screw feeders: the first one controls the biomass feeding by means of a calibrated screw speed rotation controller and the second one introduces the biomass as quick as possible into the reactor to avoid the pyrolysis in the feeding pipe. The reduced solids from the fuel reactor go to the air reactor through a fluidized bed loop seal. The oxygen carrier is oxidized in the air reactor and in the riser, and is recovered by a cyclone to be sent back to the fuel reactor. A small moving bed acts as an upper loop seal. The installation allows a perfect control of the solids circulation rate by means of a solid valve. This solid circulation rate can be also measured by a solids diverter valve.

The oxygen carrier inventory into the facility was kept steady at about 2.5 kg. Steam was used as fluidizing gas in the fuel reactor. The steam flow rate was controlled by means of a water pump that injected a known flow of water into in a vaporizer at 150ºC. A mixture of N_2 and air was fed in the air reactor. This operating method allowed an easy and accurate control of the oxygen used in the fuel reactor for syngas production.

The gas composition at the air reactor outlet stream, CO, CO_2 and O_2, was analysed in an on-line gas analyser (Siemens Ultramat 23, Oxymat 6). The gas obtained at the fuel reactor outlet was split

Submitted, accepted and published by:
Chemical Engineering Journal 405 (2021) 126679
https://doi.org/10.1016/j.cej.2020.126679

into two heated streams. The first stream was burnt with oxygen in an external reactor. The analysis of the O_2 consumed was used to calculate the oxygen demand by the syngas and helped us to better close the mass balances. CO, CO_2 and O_2 were measured at the outlet. The second stream was sent to a tar recovery system installed according to the European tar protocol [36]. CO, CO_2, H_2, and CH_4 concentrations were measured on-line after gas cleaning. A non-dispersive infrared (NDIR) analyser (Siemens Ultramat 23) was used for CH_4, CO and CO_2 measurements and an analyser based on a thermal conductivity detector (Siemens Calomat 6) for H_2. Moreover, off-line gas analyses were carried out in a gas chromatograph (CLARUS 580 Perkin Elmer) to determine the amount of C1-C5 hydrocarbons in the gas outlet stream of the fuel reactor.

Finally, an off-line method for the sampling and analysis of tars based on the European Tar Protocol [39] was used. The liquid products sampled in isopropanol were used to quantify both the water and tar contents in the gas stream. Water content was determined in a Mitsubishi Karl-Fischer titrator KF-31. Tar determination was carried out with a gas chromatograph GC-2010 Plus coupled to a mass detector QP2020 from Shimadzu. Three standards were used for external calibration: Benzene 99.8% purity, Naphthalene 99%+ purity and EPA 525 PAH MIX-A certified reference material that contains a total of 13 analytes. Furthermore, standard solutions of four different concentration levels, obtained by suitable dilutions of the standard reference, were prepared to implement the calibration.

To better know the behaviour of the oxygen carriers during the process, solid samples were extracted both from the fuel and air reactors at different operating times. These samples were physically and chemically characterized and were used to obtain information about the oxidation degree of the oxygen carrier in the two reactors, as well as the evolution of the oxygen transport capacity and reactivity with time.

2.5. Control of the oxygen used in the syngas production.

Submitted, accepted and published by:
Chemical Engineering Journal 405 (2021) 126679
https://doi.org/10.1016/j.cej.2020.126679

Since the control of the oxygen used in the syngas production is an important operating condition in the CLG process, an accurate control of the lattice oxygen reacting in the fuel reactor is necessary. In this sense, several options could be adopted to control the oxygen fed to the fuel reactor, i.e. the oxygen to biomass ratio:

- Method 1. Keeping the circulation rate of oxygen carrier at a constant value and changing the fuel feeding rate below the combustion conditions [5, 13, 26, 28]. This method produces an important change in the specific solid inventory in the fuel reactor (kg of oxygen carrier/ MW as input of energy in the biomass) and in the unit for each operating condition, and can make difficult to control the temperatures in the reactors.

- Method 2. Controlling the solid circulation rate and using typical CLC oxygen carriers diluted with an inert for a given solid circulation rate [6, 27], or even using oxygen carriers with low oxygen transport capacity. However, the different attrition rates of the materials used in the mixture could affect the composition of the mixture along the time and so the operation.

In the two above methods, the variation in the oxidation degree of the oxygen carriers is almost complete during each redox cycle.

- Method 3. Feeding into the air reactor the fixed amount of oxygen required in the fuel reactor for syngas production. This control system fits for any solid circulation rate since uncouple the heat and mass transference between air and fuel reactors, allowing an easier operation of the plant. To maintain constant the gas velocity in the air reactor at different operating conditions, dilution of the air with N_2 is necessary. This can be achieved by partial recirculation of the air reactor outlet stream, which is composed by almost pure N_2. This method for oxygen control has been satisfactorily used in previous works on Chemical Looping Reforming with both gaseous and liquid fuels [40-42] and used by first time with solid fuelled CLG in this work.

The unit was initially fed with 2.5 kg of calcined ilmenite and circulated during several hours at hot conditions in air atmosphere to clean the solids from stuck fine particles. Later, steam, air/N_2 and

Submitted, accepted and published by:
Chemical Engineering Journal 405 (2021) 126679
https://doi.org/10.1016/j.cej.2020.126679

N_2 were introduced in the fuel reactor, air reactor and loop seal, respectively, to start the operation with biomass feeding. At first, the lattice oxygen present in the 2.5 kg of calcined ilmenite produced the combustion of the biomass obtaining mostly CO_2 and H_2O at the outlet of the fuel reactor. Since a defect of oxygen was being fed in the air reactor, the concentration of CO_2 decreased progressively and the syngas production, CO and H_2, increased until reach a stable composition. In these conditions, the oxygen carrier was highly reduced both in the fuel and air reactors. The steady state conditions were maintained at least during 2 hours for each operating condition. In following days, the CLG unit was cooled and heated under N_2 atmosphere to avoid the oxidation of the oxygen carrier.

2.6. Operating parameters and data evaluation.

The main operating parameters affecting the BCLG process are the temperature of the fuel reactor, the steam to biomass ratio, S/B, and the oxygen to biomass ratio, λ. This last ratio considers the oxygen fed into the air reactor with respect to the stoichiometric oxygen needed to fully burn the biomass

$$\lambda = \frac{2F_{O2,AR,in}}{F_b \Omega_b} \quad (1)$$

where $F_{O2,AR,in}$ is the flow of O_2 fed into the air reactor (mol/h), F_b is the flow of biomass fed into the system (kg/h) and Ω_b the oxygen demand for the full combustion of the biomass (mol O/kg biomass). The total oxygen demand of the biomass is calculated considering the ultimate analysis of the biomass.

$$\Omega_b = \left(x_C \frac{32}{12} + x_H \frac{16}{2} + x_S \frac{32}{32} - x_O \right) \frac{1000}{16} \quad (2)$$

where x_i is the fraction of component i in the biomass.

The performance of the BCLG unit was evaluated based on solid fuel conversion, carbon conversion efficiency, syngas yield, and cold gas efficiency. Solid fuel or biomass conversion, X_b, is

a measurement of the amount of solid fuel converted to gas in the CLG unit, i.e. both in the fuel and air reactors,

$$X_b = \frac{F_{C,FR,out} + F_{C,AR,out}}{F_{C,b}} = \frac{F_{C,b} - F_{C,elut}}{F_{C,b}} \quad (3)$$

being

$$F_{C,b} = \frac{1000}{12} F_b x_C \quad (4)$$

$$F_{C,FR,out} = \left[F_{CO_2} + F_{CO} + F_{CH_4} + xF_{C_xH_y} \right]_{FR,out} \quad (5)$$

$$F_{C,AR,out} = F_{CO_2,AR} \quad (6)$$

$$F_{C,elut} = \frac{1000}{12} F_b x_C - (F_{C,FR,out} + F_{C,AR,out}) \quad (7)$$

Note that carbon not present in gaseous compounds corresponds to partially converted char lost by elutriation, $F_{C,elut}$, which was calculated by difference in Eq. (7).

Carbon conversion efficiency, η_{CC}, represents the fraction of the carbon converted to gas in the fuel reactor with respect to the total carbon converted to gas in the whole unit,

$$\eta_{CC} = \frac{F_{C,FR,out}}{F_{C,FR,out} + F_{C,AR,out}} \quad (8)$$

Syngas yield, Y, indicates the amount of H_2 and CO produced over the dry biomass fed into the system. It can be expressed in Nm^3/kg dry biomass.

$$Y = Y_{H2} + Y_{CO} \qquad Y_{H2} = \frac{G_{H_2}}{F_b} \qquad Y_{CO} = \frac{G_{CO}}{F_b} \quad (9)$$

where G_{H2} and G_{CO} are the gas flowrates of H_2 and CO obtained from the fuel reactor (Nm^3/h). H_2/CO ratio considers the ratio between the productions of H_2 and CO in the process. It depends on the gasifying agent used and it is useful to consider the final use of the syngas.

$$H_2 / CO = \frac{Y_{H_2}}{Y_{CO}} \quad (10)$$

Submitted, accepted and published by:
Chemical Engineering Journal 405 (2021) 126679
https://doi.org/10.1016/j.cej.2020.126679

Cold gas efficiency, η_g, represents the fraction of chemical energy contained in the product gas from the fuel reactor over the total energy of the biomass.

$$\eta_g = \frac{F_{g,FR,out}.\mathrm{LHV}_g}{\mathrm{F}_b.LHV_b}.100 \quad (11)$$

being $F_{g,FR,out}$ the molar flowrate of the gas obtained at the fuel reactor outlet (mol/h), LHV_g the low heating value of the produced gas (kJ/mol), and LHV_b the low heating value of the dry biomass (kJ/kg).

3. Results.

A total of 55 h of continuous gasification operation was carried in the 1.5 kW_{th} CLG unit using ilmenite as oxygen carrier for a total of 75 hours circulating at hot conditions. During the experimental campaign, the main operating conditions affecting the syngas production were analysed. These include the use of different gasification temperatures, T_{FR}, steam to biomass ratios, S/B, and oxygen to biomass ratios, λ. Table 3 shows the data corresponding to the different experimental conditions used in the tests carried out as well as the main results obtained describing the performance of the BCLG process.

3.1. Effect of gasification temperature.

The gasification temperature could have a relevant effect on the BCLG process, since it affects the reaction rates of the reactions taking place inside the fuel reactor. There is no consensus in the bibliography about the effect of temperature on the syngas composition. Some authors [5] observed a very high variation on gas composition with temperature in the range 700-900 ºC, meanwhile others found an optimum at 750 ºC [6] or 860 ºC [27].

In this work, the fuel reactor temperature was varied within the range 820-940 ºC that is a typical range used in previous gasification processes. Figure 3 shows the effect of fuel reactor temperature on the syngas composition using a steam-to-biomass ratio of 0.6 and an oxygen-to-biomass ratio of ≈0.3. It is seen that the gas composition (dry N_2-free basis) is hardly affected by the temperature, which agrees with the thermodynamic predictions. CO_2 was the main component, corresponding to

Submitted, accepted and published by:
Chemical Engineering Journal 405 (2021) 126679
https://doi.org/10.1016/j.cej.2020.126679

the biomass combustion. It has to be considered that some combustion of the biomass is necessary to maintain the heat balance in the whole system. CO and H_2 contents in the range of 17 vol% and 28 vol%, respectively, were obtained. It is also remarkable the high content of hydrocarbons present in the gas phase, being CH_4 the most abundant with amounts about 10%, and the rest, C2-C3, in the order of 1-2%, and 0.1-0.2%, respectively. These compounds came from the devolatilization of the biomass and no hydrocarbons higher than C3 were detected after tar condensation. Similar amounts were obtained by Wei et al. [5,13] in a 10 kW_{th} unit using saw dust as fuel and different oxygen carriers based on Fe and Fe-Ni, and by Ge et al. [27] in their 25 kW_{th} unit using rice husk as fuel and different oxygen carriers based on Ni and natural hematite. However, it should be taken into account that in all these installations the fuel reactor was a bubbling fluidized bed where the contact between the devolatilization gases and the oxygen carrier was not enough to produce the combustion or reforming of these hydrocarbons. Likely these amounts should be lower during operation in BCLG units at higher scale with improved designs. In fact, Shen et al. [28] detected lower amounts of CH_4 during coal gasification in a 5 kW_{th} CLG unit using a two-stage-based circulating bed as fuel reactor.

Figure 4 shows the effect of gasification temperature on the different gasification performance parameters. Except when no water was used for fluidization, S/B ratio of 0.05, biomass conversion was very high, X_b>90%, in the whole range of temperatures. It can be seen that an increase in the gasification temperature produced an increase in the carbon conversion efficiency, reaching values close to 100% at 940ºC. These values could be even higher in larger scale units implemented with carbon stripper reactors. This result demonstrated that BCLG process would allow zero CO_2 emissions to the atmosphere, one of the advantages of this technology versus the Dual Fluidized Bed Gasification (DFBG) process. Finally, an increase in the temperature increased the values of syngas yield and cold gas efficiency, in the order of 5-10%. This fact can be explained by the increase in the reaction rate of all the reactions taking place in the fuel reactor with increasing temperature.

3.2. Effect of oxygen-to-fuel ratio.

Submitted, accepted and published by:
Chemical Engineering Journal 405 (2021) 126679
https://doi.org/10.1016/j.cej.2020.126679

The oxygen-to-fuel ratio, λ, is the main operating variable affecting the process since it represents the amount of oxygen used for gasification/combustion and therefore for syngas production. However, this parameter is also very important to fulfil the heat balance in the system, that is, to reach autothermal conditions. As above mentioned, there are several possibilities to control the oxygen-to-fuel ratio, although the used method in this work is the only one that would allow a comparison of this parameter without affecting other fluid dynamics parameters on the CLG unit.

Figure 5 shows the gas composition as a function of λ, at 940ºC and a steam-to-biomass ratio of 0.6. As can be seen, CO and H_2 concentrations decreased with increasing λ. In contrast, CO_2 concentration significantly increased. This was because more lattice oxygen was available to react with biomass devolatilization and reforming gases, increasing the contribution of the combustion reactions, (R4)-(R6) and (R8)-(R10), over the gasification R(2)-R(3), partial combustion, R(7), R(11), and reforming ones R(12), R(13), R(16). Therefore, it is concluded that the best syngas composition was obtained at low λ values.

It is remarkable, in contrast to what happened with the CO and H_2, that the amount of hydrocarbons, C1-C3, remained almost constant with λ. This fact could mean that the contact time or the reaction rate of the ilmenite with these hydrocarbons coming from the biomass devolatilization were not high enough to burn or to reform them. In fact, Abad et al. [43] found a lower reactivity of ilmenite with CH_4 and CO than with H_2.

Figure 6 shows the effect of λ on the gasification parameters obtained at 940ºC and S/B=0.6. As can be seen in Table 3, similar results were obtained at other temperatures and steam-to-biomass ratios. Almost independently of the λ used, very high values of biomass conversion efficiency, X_b>90%, were obtained in all cases except when no water was used for fluidization (see below). Most of the carbon contained in the biomass was converted into syngas in the fuel reactor, as can be seen through the η_{cc} parameter, which reached values close to 100% in the majority of conditions. The variation in syngas composition with λ affected especially to the syngas yield, *Y*, and to the cold

Submitted, accepted and published by:
Chemical Engineering Journal 405 (2021) 126679
https://doi.org/10.1016/j.cej.2020.126679

gas efficiency, η_g, which decreased with increasing λ. At T_{FR}=940ºC and S/B=0.6 the syngas yield and the cold gas efficiency decreased 32% and 15%, respectively, when λ varied from 0.15 to 0.35.

The same tendencies found in this work were obtained by other researchers using other methods for the control of the oxygen used for syngas production [6, 27]. An increase of combustion reactions led always to the transformation of CO and H_2 into CO_2 and H_2O. However, the oxygen-to-fuel ratio used is very important to reach autothermal conditions in the global process, as it was previously remarked on. Preliminary heat balances carried out at T_{FR}=850-950ºC, S/B=0.15-0.6 and using the typical gas compositions obtained in this work indicated that the autothermic process is reached at oxygen-to-fuel ratios, λ≈0.26-0.30, depending on the operating conditions and temperature of preheated streams. Considering the high unconverted hydrocarbons usually obtained in most of the tests, a syngas composed by 37-40 % CO_2; 27-30% H_2; 17-21% CO; 10-12% CH_4; and 2-3% C2-C3 could be obtained at autothermal conditions (λ=0.28). This composition would correspond approximately to a syngas yield of 0.65 Nm3/kg dry biomass and a cold gas efficiency of 76 %. These values would improve if hydrocarbons coming from biomass devolatilization could be converted inside the fuel reactor.

3.3. Effect of steam to biomass ratio.

In the BCLG process, steam is usually used as gasifying agent and as fluidizing gas in the fuel reactor. It has to be considered that the amount of steam has a strong effect on the gasification and reforming reactions and on the heat balance of the BCLG process since the production of steam consumes a high amount of energy. Figure 7 shows the effect of the steam-to-biomass ratio on the gas composition at 880 ºC and a λ value of ≈0.3. A reference test using pure N_2 for fluidization in the fuel reactor is included. In this test, the steam introduced (S/B=0.05) corresponded only to the moisture of the biomass. It is observed in the Figure, and in general in the Table 3, that an increase in the S/B ratio from 0.05 to 0.9 produced an increase in the H_2 and CO_2 concentrations and a decrease in the CO concentration. Obviously, the increase in the S/B ratio produced an increase in

Submitted, accepted and published by:
Chemical Engineering Journal 405 (2021) 126679
https://doi.org/10.1016/j.cej.2020.126679

the H_2/CO ratio, ranging from ≈1 to ≈1.5 (see Figure 8). These effects were a consequence of the increase in the char gasification and reforming reaction rates with increasing the S/B ratio but also to the effect of the water gas shift reaction. It has to be mentioned that the tests at S/B=0.9 were carried out a lower biomass feeding rate in order to maintain the gas velocities inside the fuel reactor and to avoid excessive char elutriation.

Figure 9 shows the effect of the steam-to-biomass ratio on the gasification parameters. It can be seen that the addition of steam produced an improvement in the biomass conversion, although high values, X_b>90%, were always obtained, except in the tests where N_2 was used for fluidization. Also, very high carbon conversion efficiencies were obtained in all cases, η_{cc}>90%, and especially at the highest temperature used (940 ºC), η_{cc}>95%, which meant that a good char gasification reaction took place in the fuel reactor, with low char amount passing to the air reactor.

The most significant effect of the steam addition happened on the syngas yield and cold gas efficiency. In both cases, improvements up to 50% (20 points) were observed when S/B ratio varied from 0.05 to 0.9, since more biomass was gasified in the fuel reactor. However, a small effect of increasing H_2O content on the reforming of CH_4 and other hydrocarbons (C2-C3) was also observed, since similar concentrations of these compounds were found at the fuel reactor outlet at the different S/B ratios (see Figure 7). This fact should be considered in the mass and heat balance since the heat necessary to evaporate the H_2O could be an important fraction of the heat needed in the global system. In this sense, the possibility to use CO_2 or mixtures H_2O/CO_2 was analysed by Shen et al. [28], although they found that steam was the preferred gasifying agent. In addition, a syngas highly concentrated in CO_2 could be obtained, which can be harmful if this stream is used in a Fischer-Tropsch process.

3.4. Tar content.

A relevant aspect of the gasification processes for the production of liquid fuels via Fischer-Tropsch is the cleaning section. The syngas produced by any gasification process should be as clean

Submitted, accepted and published by:
Chemical Engineering Journal 405 (2021) 126679
https://doi.org/10.1016/j.cej.2020.126679

as possible in order to decrease the energy and economic cost of that section. In this sense, one of the advantages of CLG with respect to other gasification processes is the lower amount of tars produced. It has been demonstrated that the presence of the oxygen carrier contributes not only to the biomass conversion but also to the tar content reduction [25,44,45].

A dedicated study about the tar generation during the CLG process using ilmenite as oxygen carrier was carried out in this work. Figure 10 shows the amount of tar generated as a function of the steam-to-biomass ratio for several temperatures, including tests with different oxygen-to-fuel ratios. It was observed that an increase in the fuel reactor temperature or in the steam-to-biomass ratio produced always a decrease in the amount of tar generated. In the first case, as a consequence of an increase in the tar cracking, (R15), or tar combustion with the oxygen carrier, (R17)-(R18), and in the second one, due to a higher relevance of the tar reforming reaction, (R16), where oxygen carrier acts as a catalyst.

Up to our best knowledge, no data exist in the literature about tar generation in continuous operation BCLG units. In this work, values below 2.2 g/kg dry biomass were found for typical conditions corresponding to BCLG, which are lower to the previously reported in other gasification processes. Since the gas yield is about 1-1.3 Nm^3/kg dry biomass in the majority of the operating conditions, the above values correspond to tar values below 2 g/Nm^3 dry N_2-free basis, that it is another usual way to represent the tar generation. In a previous work [25], a study about tar formation in biomass indirect gasification (also known as dual fluidized bed gasification, DFBG) of pine wood was carried out in the same installation herein used for the BCLG tests. Silica sand as a reference material, olivine, and olivine impregnated with Fe were used as bed materials. Compared to the ≈17 g/Nm^3 obtained with silica sand, the use of olivine reduced the amount of tar generated to values from 5.1-8.3 g/Nm^3, and to 2.6-4.2 g/Nm^3 when using the Fe-olivine material. According to the results showed in Figure 10, it is demonstrated that the use of an oxygen carrier in BCLG produces a relevant decrease in the amount of tar generation.

Submitted, accepted and published by:
Chemical Engineering Journal 405 (2021) 126679
https://doi.org/10.1016/j.cej.2020.126679

Figure 11 shows the distribution of the different tar compounds determined in all the tests. It is observed that tar compounds distribution was similar for all the tests carried out under different operation conditions. In all cases, the major compounds detected were naphthalene (63%-79%), indene (5%-15%), byphenil (1%-6%) and phenanthrene (1%-3%). Low concentration of benzene was determined (≈0.05 g/kg dry biomass).

3.5. Attrition of ilmenite under BCLG

The fluid-dynamic behavior of the materials used in a fluidized bed represents an important indicator of the suitability of any material to be used in a CLG process. It should be remembered that, according to the method herein used to control the oxygen used in the syngas production, the oxygen carrier is highly reduced in the fuel reactor. This could have relevant consequences in some oxygen carriers if the reduced materials are prone to agglomerate. It is noticeable that no defluidization or agglomeration was observed for any of the experiments carried out with ilmenite as oxygen carrier under CLG conditions.

Another relevant aspect to consider in the CLG process is the attrition behavior and lifetime of the particles considering their special features. Figure 12 shows the experimental attrition rate of the ilmenite during the 75 hours of operation on the CLG continuous unit, 55 of them corresponding at biomass gasification. These values correspond to the fine particles, with a size lower than 40 μm, recovered during operation in the cyclones located downstream the fuel and air reactors. An average attrition rate value of 0.16 wt%/h was obtained, which corresponds to a lifetime of 630 h. In contrast, Cuadrat et al. [46], using the same ilmenite, observed an attrition rate value of 0.064%/h after 40 hours of operation under CLC conditions, which corresponds to a lifetime of 1300 h. The more extreme conditions undergone by the oxygen carrier in CLG reduced the lifetime of the particles by a half compared with CLC. This also led a decrease in the oxygen transport capacity of the material, $R_{o,oc}$ from 4.03 in the fresh particles to 3.77 after operation.

3.6. SEM-EDX characterization.

Submitted, accepted and published by:
Chemical Engineering Journal 405 (2021) 126679
https://doi.org/10.1016/j.cej.2020.126679

Samples of ilmenite were extracted from the fuel and air reactors during operation in order to know the evolution of the material with operating time. Figure 13 shows the SEM images of the entire particles, as well as of the internal part of the particles. Although in general the aspect of the entire ilmenite particles was good, some cracks appeared on the outer part of the used particles and, as a consequence, particles with some parts of the external shell broke away after the operation were also observed.

The internal view of the cut-off ilmenite particles showed the formation of a layer in the outer part of most of the particles, and, in some cases, these shells were broken away from them during operation in the fluidized bed. A more detailed view of the external part of particles showed the shell growing and how this shell was being separated from the particle after several operating hours. This fact could be explained in terms of the great changes in the structure that the ilmenite particles underwent during the redox reactions.

To determine the reasons for the outer layer formation, an EDX study was carried out to some of the particles (see Figure 14). The outer layer was not observed in the calcined particles and a good distribution of Fe inside the particles was observed. In contrast, the particles used during 75 hours of operation showed that the outer shell was enriched in iron, indicating the migration of this metal from the inner to the external part of the particle during BCLG operation. This fact was also observed in previous studies during the use of ilmenite in CLC processes [46]. This iron migration could be higher in the BCLG process due to the more extreme reducing conditions here existing, which led to an increase in the attrition rate and a lower lifetime of the particles, as above mentioned.

3.7. Solid conversion of ilmenite under BCLG conditions

The high reducing conditions existing in the fuel reactor and the method herein used for the control of the oxygen used for syngas production made necessary to analyse how the ilmenite was present in the system. Therefore, solid samples collected from the fuel and air reactors during operation were analysed by several techniques.

Submitted, accepted and published by:
Chemical Engineering Journal 405 (2021) 126679
https://doi.org/10.1016/j.cej.2020.126679

XRD analysis showed that main crystal Fe phases present in the solid were Fe_3O_4, $FeTiO_3$, and Fe_2TiO_4. FeO was found (low concentration) only in test 17 and metallic Fe and Fe_2O_3 were never detected. These results would confirm that the samples extracted from both air and fuel reactors were highly reduced, with Fe_3O_4 and $FeTiO_3$ as the main Fe compounds. Magnetite is a cubic phase in which 24 out of 56 atoms in its unit cell are Fe cations: 16 of them as Fe^{3+} and 8 as Fe^{2+}. $FeTiO_3$ would be the main Fe reduced phase because Fe_2TiO_4 phase was found in lower concentration. These results are referred to the crystalline compounds but all the samples presented about 20% of amorphous, determined by semiquantitative method (S-Q).

In addition, temperature programmed oxidation (TPO) tests were carried out. Figure 15 shows the oxidation level of the ilmenite as a function of the λ parameter, assuming the limits corresponding to the oxygen carrier fully oxidized (Fe_2TiO_5+Fe_2O_3) and fully reduced ($FeTiO_3$+Fe_3O_4).

It can be seen that the ilmenite particles presented a high level of reduction, especially in the fuel reactor, and at low values of λ. Oxidation levels below 35% were detected in most of the samples both in the fuel and air reactors. These phenomena could be responsible of the lower lifetime found for ilmenite under BCLG conditions in relation to their performance in CLC. In spite of this result, ilmenite maintained a high reactivity after the operation and could be considered as a suitable oxygen carrier for BCLG.

4. Conclusions

The behaviour of ilmenite as oxygen carrier for the BCLG process was investigated during 55 h of pine wood gasification in a 1.5 kW_{th} BCLG unit. A novel method for controlling the oxygen fed in the air reactor for ilmenite oxidation has demonstrated to be an accurate method to control the lattice oxygen used for syngas production in the fuel reactor.

The high biomass conversions, X_b>86%, and carbon conversion efficiencies, η_{cc}>90%, obtained demonstrated the high CO_2 capture inherent to the BCLG processes. The most relevant variable affecting syngas quality and, therefore, the syngas yield and cold gas efficiency, was the oxygen to

biomass ratio, λ. Since a compromise between combustion and gasification reactions should be considered to reach autothermal BCLG operation a syngas with high CO_2 content was obtained. CH_4 contents in the order of 10 vol% were also obtained proceeding from the unburnt volatiles although syngas quality will highly improve after hydrocarbons conversion. It is noteworthy the low tar contents generated, below 3 g/kg dry biomass (< 2 g/Nm^3 d.b.), which represents a clear advantage of BCLG with respect to other syngas production processes.

The characterization of ilmenite after BCLG operation showed a reduction of lifetime with respect to CLC conditions mainly due to the highly reduced state of the oxygen carrier in the fuel reactor. Regardless, ilmenite can be considered as a suitable oxygen carrier to be used in BCLG processes for high quality syngas production without CO_2 emissions to the atmosphere.

Acknowledgements

This work has been supported by the framework of the European Union's Horizon 2020 - Research and Innovation Framework Programme under grant agreement No 817841 (Chemical Looping gasification for sustainable production of biofuels - CLARA), and by the AEI/FEDER, UE (ENE2017-89473R).

References

[1] V.S. Sikarwar, M. Zhao, P.S. Fennell, N. Shah, E.J. Anthony, Progress in biofuel production from gasification, Prog. Energy Combust. Sci. 61 (2017)189-248.

[2] C. Higman, M. van der Burgt, Gasification: Second Edition, Elsevier Inc. (2008).

[3] T. Mendiara, F. García-Labiano, A. Abad, P. Gayán, L.F. de Diego, M.T. Izquierdo, J. Adánez, Negative CO_2 emissions through the use of biofuels in chemical looping technology: A review, App. Energy 232 (2018) 657-684.

[4] X. Zhao, H. Zhou, V.S. Sikarwar, M. Zhao, A.H.A. Park, P.S. Fennell, L. Shen, L.S. Fan, Biomass-based chemical looping technologies: the good, the bad and the future, Energy Environ. Sci. 10 (2017) 1885-1910.

[5] G. Wei, F. He, Z. Huang, A. Zhen, K. Zhao, H. Li, Continuous Operation of a 10 kW_{th} Chemical Looping Integrated Fluidized Bed Reactor for Gasifying Biomass Using an Iron-Based Oxygen Carrier, Energy Fuels 29 (2015) 233-241.

[6] H. Ge, L. Shen, F. Feng, S. Jiang, Experiments on biomass gasification using chemical looping with nickel-based oxygen carrier in a 25 kW_{th} reactor, App. Thermal Eng. 85 (2015) 52-60.

[7] J. Adánez, A. Abad, T. Mendiara, P. Gayán, L.F. de Diego, F. García-Labiano, Chemical looping combustion of solid fuels, Prog. Energy Combust. Sci. 65 (2018) 6-66.

[8] A. Lyngfelt, Oxygen carriers for chemical looping combustion. 4000 h of operational experience. Oil Gas Sci. Technol. 66 (2011)161–172.

[9] Z. Huang, F. He, H. Zhu, D. Chen, K. Zhao, G. Wei, Y. Feng, A. Zheng, Z. Zhao, H. Li, Thermodynamic analysis and thermogravimetric investigation on chemical looping gasification of biomass char under different atmospheres with Fe_2O_3 oxygen carrier, App. Energy 157 (2015) 546-553.

[10] Z. Hu, X. Ma, E. Jiang, The effect of microwave pretreatment on chemical looping gasification of microalgae for syngas production, Energy Conv. Manag. 143 (2017) 513-521.

[11] D. Xu, Y. Zhang, T.L. Hsieh, M. Guo, L. Qin, C. Chung, L.S. Fan, A. Tong, A novel chemical looping partial oxidation process for thermochemical conversion of biomass to syngas, App. Energy 22 (2018) 119-131.

[12] Z. Li, H. Xu, W. Yang, M. Xu, F. Zhao, Numerical investigation and thermodynamic analysis of syngas production through chemical looping gasification using biomass as fuel, Fuel 246 (2019) 466-475.

[13] G. Wei, F. He, Z. Zhao, Z. Huang, A. Zhen, K. Zhao, H. Li, Performance of Fe–Ni bimetallic oxygen carriers for chemical looping gasification of biomass in a 10 kW_{th} interconnected circulating fluidized bed reactor, Int. J. Hydrog. Energy 40 (2015) 16021-16032.

[14] Z. Huang, Z. Deng, F. He, D. Chen, G. Wei, K. Zhao, A. Zheng, Z. Zhao, H. Li, Reactivity investigation on chemical looping gasification of biomass char using nickel ferrite oxygen carrier, Int. J. Hydrog. Energy 42 (2017) 14458-14470.

[15] F. He, Z. Huang, G. Wei, K. Zhao, G. Wuang, X. Kong, Y. Feng, H. Tan, S. Hou, Y. Lv, G. Jiang, Y. Guo, Biomass chemical-looping gasification coupled with water/CO_2-splitting using $NiFe_2O_4$ as an oxygen carrier, Energy Conv. Manag. 201 (2019) 122157.

[16] Y. Lin, H. Wang, Z. Huang, M. Liu, G. Wei, Z. Zhao, H. Li, Y. Fang, Chemical looping gasification coupled with steam reforming of biomass using $NiFe_2O_4$: Kinetic analysis of DAEM-TI, thermodynamic simulation of OC redox, and a loop test, Chem. Eng. J. 395 (2020): 125046.

[17] G. Wei, F. He, W. Zhao, Z. Huang, K. Zhao, Z. Zhao, A. Zheng, X. Wu, H. Li, Experimental Investigation of Fe−Ni−Al Oxygen Carrier Derived from Hydrotalcite-like Precursors for the Chemical Looping Gasification of Biomass Char, Energy Fuels 31 (2017) 5174-5182.

[18] Y. Ma, H. Zhao, P. Niu, J. Ma, Using Synthetic Cu-Fe Metal Oxides as Oxygen Carriers in Biomass Chemical-looping Gasification, 4th International Conference on Chemical Looping, September 26-28 (2016), Nanjing, China.

[19] P. Niu, Y. Ma, X. Tian, J. Ma, H. Zhao, Chemical looping gasification of biomass: Part I. screening Cu-Fe metal oxides as oxygen carrier and optimizing experimental conditions, Biomass Bioenergy 108 (2018) 146-156.

[20] X. Tian, P. Niu, Y. Ma, H. Zhao, Chemical-looping gasification of biomass: Part II. Tar yields and distributions, Biomass Bioenergy 108 (2018) 178-189.

[21] Y. Wu, Y. Liao, G. Liu, X. Ma, Syngas production by chemical looping gasification of biomass with steam and CaO additive, Int. J. Hydrog. Energy 43 (2018) 19375-19383.

[22] J. Wu, L. Bai, H. Tian, J. Riley, R. Siriwardane, Z. Wang, T. He, J. Li, J. Zhang, J. Wu, Chemical looping gasification of lignin with bimetallic oxygen carriers, Int. J. Greenhouse Gas Control 93 (2020) 102897.

[23] Q. Hu, Y. Shen, J. W. Chew, T. Ge, C.-H. Wang, Chemical looping gasification of biomass with Fe_2O_3/CaO as the oxygen carrier for hydrogen-enriched syngas production, Chem. Eng. J. 379 (2020) 122346.

[24] J. Yan, R. Sun, L. Shen, H. Bai, S. Jiang, Y. Xiao, T. Song, Hydrogen-rich syngas production with tar elimination via biomass chemical looping gasification (BCLG) using $BaFe_2O_4/Al_2O_3$ as oxygen carrier, Chem. Eng. J. 387 (2020) 124107.

[25] M. Virginie, J. Adánez, C. Courson, L.F. de Diego, F. García-Labiano, D. Niznansky, A. Kiennemann, P. Gayán, A. Abad, Effect of Fe–olivine on the tar content during biomass gasification in a dual fluidized bed, App. Catal. B: Environ. 121-122 (2012) 214-222.

[26] S. Huseyin, G. Wei, H. Li, F. He, Z. Huang, Chemical-looping gasification of biomass in a 10 kW_{th} interconnected fluidized bed reactor using Fe_2O_3/Al_2O_3 oxygen carrier, J. Fuel Chem. Technol. 42 (2014) 922-931.

[27] H. Ge, W. Guo, L. Shen, T. Song, J. Xiao, Biomass gasification using chemical looping in a 25 kW_{th} reactor with natural hematite as oxygen carrier, Chem. Eng. J. 286 (2016) 174-183.

[28] T. Shen, J. Wu, L. Shen, J. Yan, S. Jiang, Chemical Looping Gasification of Coal in a 5 kW_{th} Interconnected Fluidized Bed with a Two-Stage Fuel Reactor, Energy Fuels 32 (2018) 4291−4299

[29] A. Cuadrat, A. Abad, F. García-Labiano, P. Gayán, L.F. de Diego, J. Adánez, Relevance of the coal rank on the performance of the in situ gasification chemical-looping combustion. Chem. Eng. J. 195–196 (2012) 91–102

[30] R. Pérez-Vega, A. Abad, F. García-Labiano, P. Gayán, L.F. de Diego, J. Adánez, Coal combustion in a 50 kW_{th} chemical looping combustion unit: seeking operating conditions to maximize CO_2 capture and combustion efficiency, Int. J. Greenhouse Gas Control 50 (2016) 80-92.

[31] N. Berguerand, A. Lyngfelt, The use of petroleum coke as fuel in a 10 kW_{th} chemical-looping combustor, Int. J. Greenhouse Gas Control 2 (2008) 169-179.

[32] P. Markström, C. Linderholm, A. Lyngfelt, Chemical-looping combustion of solid fuels – design and operation of a 100kW unit with bituminous coal, Int. J.Greenhouse Gas Control 15 (2013) 150-162.

[33] A. Thon, M. Kramp, E.U. Hartge, S. Heinrich, J. Werther, Operational experience with a system of coupled fluidized beds for chemical looping of solid fuels using ilmenite as oxygen carrier, App. Energy 118 (2014) 307-317.

[34] J. Ströhle, M. Orth, B. Epple, Chemical looping combustion of hard coal in a 1 MW_{th} pilot plant using ilmenite as oxygen carrier, App. Energy 157 (2015) 288-294.

[35] H. Thunman, F: Lind, C. Breitholtz, N. Berguerand, M. Seeman, Using an oxygen-carrier as bed material for combustion of biomass in a 12-MW_{th} circulating fluidized-bed boiler, Fuel 113 (2013) 900-909.

[36] B.A. Anderson, F. Lind, A. Corcoran, H. Thunman, 4000 hours of operation with oxygen carriers in industrial relevant scale (75 MW_{th}), 4th Int. Conf. on chemical looping (2016)

[37] F. Lind, M. Seemann, H. Thunman, Continuous Catalytic Tar Reforming of Biomass Derived Raw Gas with Simultaneous Catalyst Regeneration, Ind. Eng. Chem. Res. 50 (2011) 11553–11562.

[38] Y. Shen, K. Yoshikawa, Recent progresses in catalytic tar elimination during biomass gasification or pyrolysis—A review, Renew. Sustain. Energy Rev.21 (2013) 371–392.

[39] P. Simell, P. Ståhlberg, E. Kurkela, J. Albrecht, S. Deutsch, K. Sjöström, Provisional protocol for the sampling and analysis of tar and particulates in the gas from large-scale biomass gasifiers. Version 1998, Biomass Bioenergy 18 (2000) 19-38.

[40] L.F. de Diego, M. Ortiz, F. García-Labiano, J. Adánez, A. Abad, P. Gayán, Hydrogen production by chemical-looping reforming in a circulating fluidized bed reactor using Ni-based oxygen carriers, J. Power Sources 192 (2009) 27-34.

[41] T. Pröll, J. Bolhàr-Nordenkampf, P. Kolbitsch, H. Hofbauer, Syngas and a separate nitrogen/argon stream via chemical looping reforming – A140 kW pilot plant study. Fuel 89 (2010) 1249–1256.

[42] E. García-Díez, F. García-Labiano, L.F. de Diego, A. Abad, P. Gayán, J. Adánez, J.A.C. Ruíz, Steam, dry, and steam-dry chemical looping reforming of diesel fuel in a 1 kW_{th} unit, Chem. Eng. J. 325 (2017) 369-377.

[43] A. Abad, J. Adánez, A. Cuadrat, F. García-Labiano, P. Gayán, L.F. de Diego, Kinetics of redox reactions of ilmenite for chemical-looping combustion, Chem. Eng. Sci. 66 (2011) 689-702.

[44] Z. Huang, F. He, Y. Feng, R. Liu, K. Zhao, A. Zheng, S. Chang, Z. Zhao, H. Li. Characteristics of biomass gasification using chemical looping with iron ore as an oxygen carrier, Int. J. Hydrog. Energy 38 (2013) 14568-14575.

[45] A. Sarvaramini, F. Larachi, Catalytic oxygen less steam cracking of syngas containing benzene model tar compound over natural Fe-bearing silicate minerals, Fuel 97 (2012) 741-750.

[46] A. Cuadrat, A. Abad, J. Adánez, L.F. de Diego, F. García-Labiano, P. Gayán, Behaviour of ilmenite as oxygen carrier in chemical-looping combustion, Fuel Process. Technol. 94 (2012) 101-112.

Submitted, accepted and published by:
Chemical Engineering Journal 405 (2021) 126679
https://doi.org/10.1016/j.cej.2020.126679

Tables

Table 1. Physical properties of the calcined ilmenite.

XRD composition	Fe_2TiO_5, Fe_2O_3, TiO_2
Particle diameter (µm)	100-300
True density (kg/m^3)	4100
Crushing strength (N)	2.2
Porosity (%)	1.2
BET Surface (m^2/g)	0.8

Submitted, accepted and published by:
Chemical Engineering Journal 405 (2021) 126679
https://doi.org/10.1016/j.cej.2020.126679

Table 2. Pine wood biomass composition (wet basis).

Proximate analysis (wt%)	
Moisture	5.6
Ashes	0.6
Volatile matter	78.5
Fixed carbon	15.3
Ultimate analysis (wt%)	
C	49.7
H	6.3
N	0.1
S	0.0
O (by difference)	37.7
Low Heating Value, LHV (kJ/kg)	17434
Ω_b (mol O/kg wet biomass)	90.85

Submitted, accepted and published by:
Chemical Engineering Journal 405 (2021) 126679
https://doi.org/10.1016/j.cej.2020.126679

Table 3. Biomass gasification tests carried out in the 1.5 kW_{th} CLG unit. Operating variables: gasification temperature (T_{FR}), steam-to-biomass ratio (S/B), and oxygen-to-biomass ratio (λ). Gasification parameters: solid fuel conversion (X_b), carbon conversion efficiency (η_{cc}), syngas yield (Y), and cold gas efficiency (η_g).

Test	T_{FR}	S/B	λ	Gas composition (dry and N_2 free, vol%)					X_b	η_{cc}	Y	η_g	H_2/CO
	°C	kg/kg	-	CO_2	CO	H_2	CH_4	C_{2-3}	(%)	(%)	(Nm^3/kg)	(%)	
1	820	0.05	0.30	41.8	22.7	18.4	13.0	4.1	79.8	88.4	0.34	54.0	0.8
2	820	0.6	0.27	36.9	19.5	25.7	13.7	4.1	90.6	88.4	0.46	70.4	1.3
3	820	0.6	0.36	42.9	16.0	26.5	10.9	3.7	95.1	91.7	0.48	68.1	1.7
4	820	0.9	0.24	31.1	19.5	32.7	13.2	3.5	99.8	93.0	0.69	91.5	1.7
5	820	0.9	0.48	50.4	13.5	20.7	12.7	2.7	98.8	91.9	0.38	61.0	1.5
6	880	0.05	0.18	19.4	33.2	30.7	13.8	2.8	78.3	93.3	0.65	77.9	0.9
7	880	0.05	0.33	44.9	21.7	18.9	12.0	2.5	86.8	96.0	0.41	57.5	0.9
8	880	0.6	0.18	27.8	20.7	39.7	10.1	1.8	95.4	96.3	0.89	92.9	1.9
9	880	0.6	0.33	41.1	19.0	26.7	10.2	2.7	92.8	97.5	0.55	69.5	1.4
10	880	0.9	0.15	32.3	19.0	33.5	11.6	3.6	98.0	98.1	0.72	92.5	1.8
11	880	0.9	0.30	36.8	19.3	27.7	14.0	2.3	96.6	97.4	0.59	81.0	1.4
12	880	0.9	0.30	39.2	18.7	27	12.4	2.7	97.5	97.4	0.57	77.5	1.4
13	880	0.9	0.30	37.2	17.7	30.2	12.3	2.6	94.3	96.3	0.60	78.2	1.7
14	880	0.9	0.46	49.0	15.6	19.4	12.1	3.8	99.2	96.8	0.40	66.8	1.3
15	940	0.05	0.15	16.8	35.7	34.1	11.6	1.9	65.9	97.1	0.66	68.9	1.0
16	940	0.05	0.30	33.4	29.2	25.0	10.8	1.6	81.0	95.4	0.55	61.4	0.9
17	940	0.6	0.15	27.8	21.1	39.9	9.4	1.7	89.5	98.5	0.87	88.0	1.9
18	940	0.6	0.34	42.4	16.9	27.2	10.1	3.4	95.7	98.9	0.55	72.8	1.6

Submitted, accepted and published by:
Chemical Engineering Journal 405 (2021) 126679
https://doi.org/10.1016/j.cej.2020.126679

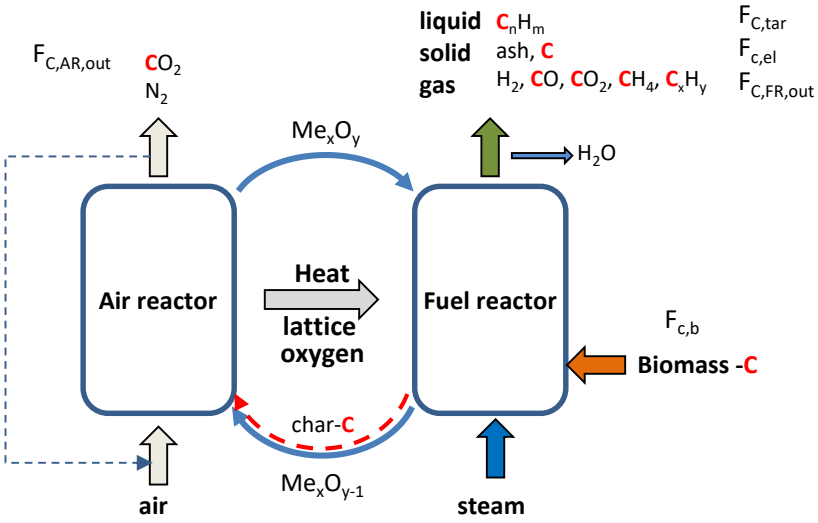

Figure 1. Schematic illustration of Biomass Chemical Looping Gasification process. Me_xO_y denotes a metal oxide and Me_xO_{y-1} its reduced compound in the oxygen carrier.

Submitted, accepted and published by:
Chemical Engineering Journal 405 (2021) 126679
https://doi.org/10.1016/j.cej.2020.126679

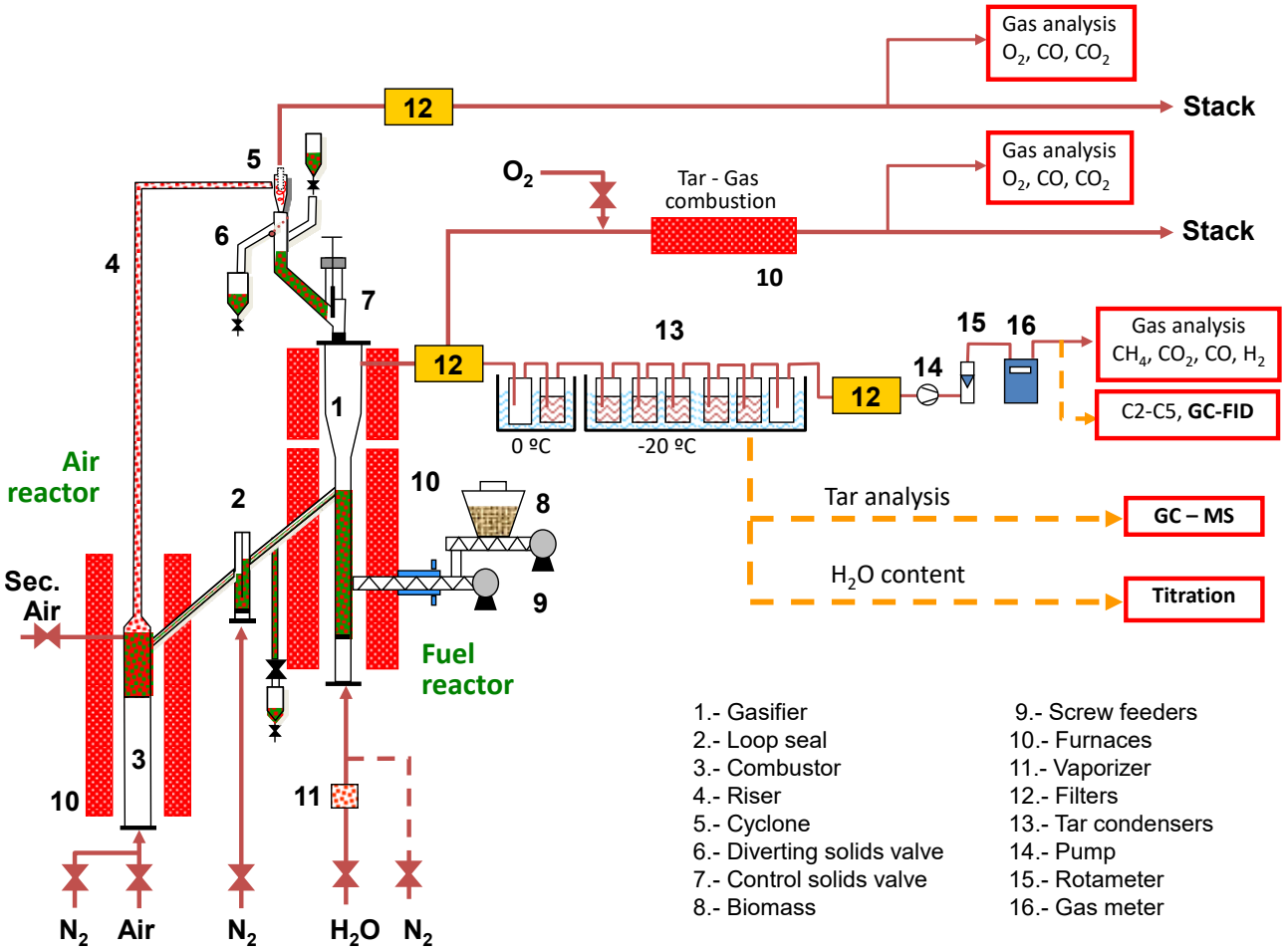

Figure 2. Scheme of the 1.5 kW_{th} CLG unit at ICB-CSIC.

Submitted, accepted and published by:
Chemical Engineering Journal 405 (2021) 126679
https://doi.org/10.1016/j.cej.2020.126679

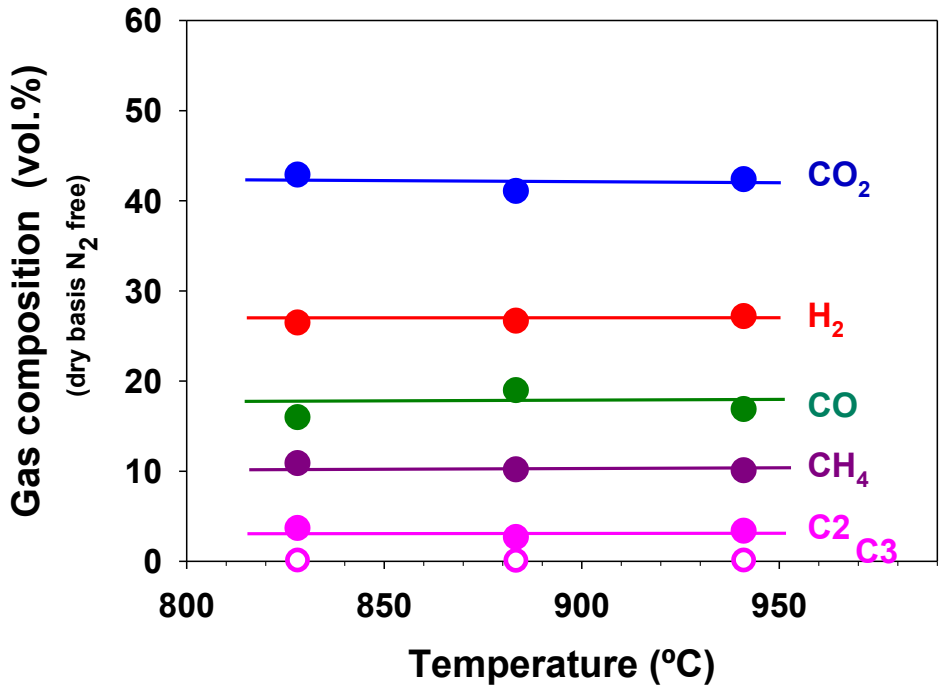

Figure 3. Effect of the fuel reactor temperature, T_{FR}, on syngas composition. Steam-to-biomass ratio, S/B=0.6; oxygen-to-biomass ratio, λ≈0.3.

Submitted, accepted and published by:
Chemical Engineering Journal 405 (2021) 126679
https://doi.org/10.1016/j.cej.2020.126679

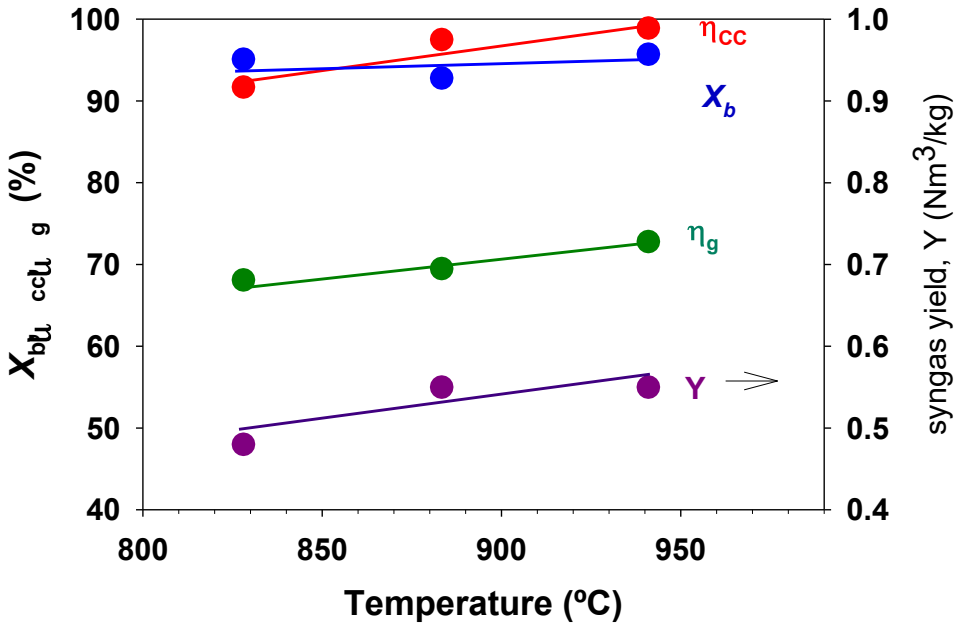

Figure **4**. Effect of the fuel reactor temperature, T_{FR}, on biomass conversion (X_b), carbon conversion efficiency (η_{cc}), cold gas efficiency (η_g), and syngas yield (Y). Steam-to-biomass ratio, S/B=0.6; oxygen-to-biomass ratio, λ≈0.3.

Submitted, accepted and published by:
Chemical Engineering Journal 405 (2021) 126679
https://doi.org/10.1016/j.cej.2020.126679

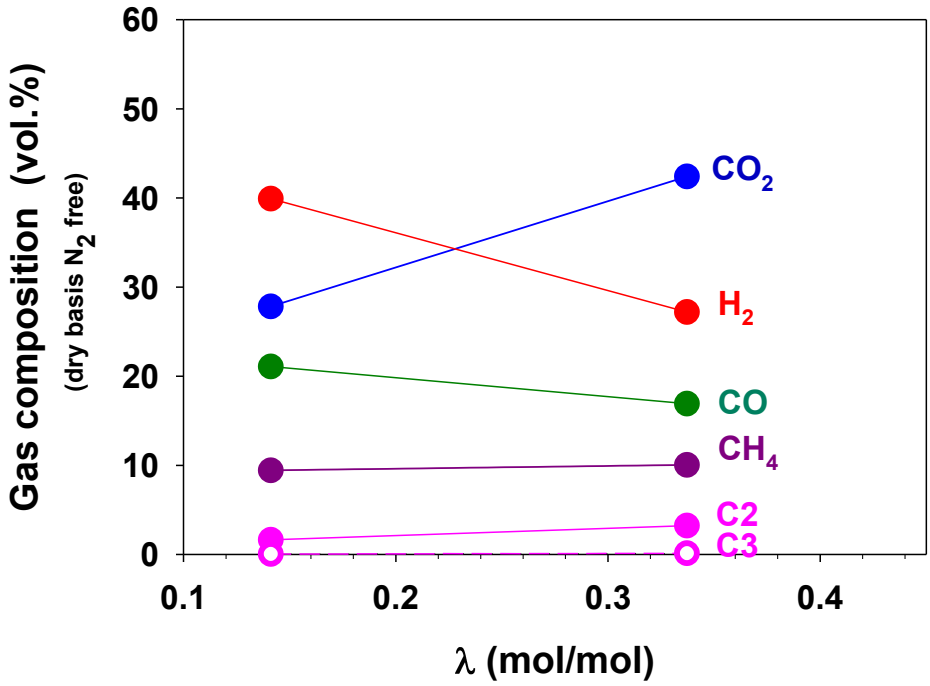

Figure 4. Effect of oxygen-to-fuel ratio, λ, on gas composition. Temperature, T_{FR}=940 ºC; steam-to-biomass ratio, S/B=0.6.

Submitted, accepted and published by:
Chemical Engineering Journal 405 (2021) 126679
https://doi.org/10.1016/j.cej.2020.126679

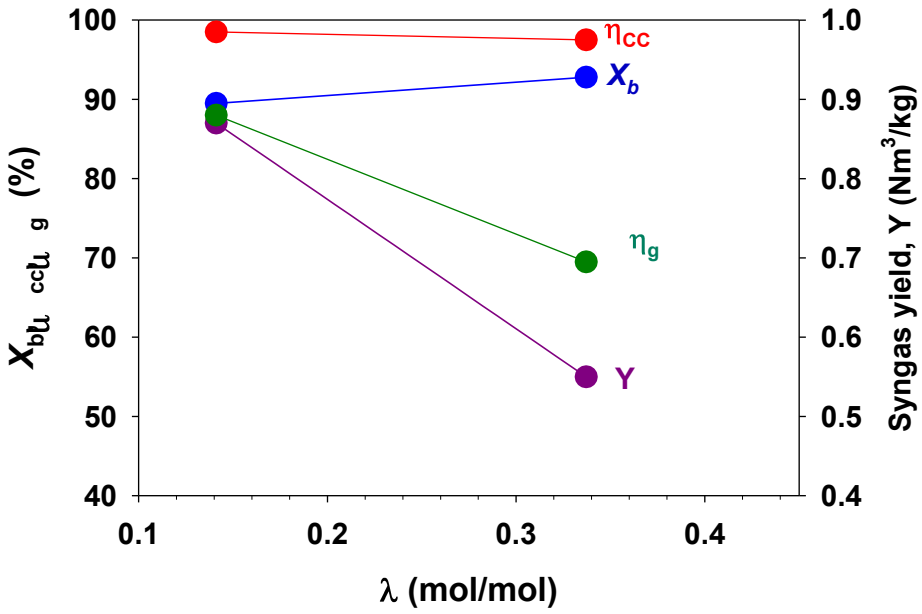

Figure 6. Effect of oxygen-to-fuel ratio, λ, on biomass conversion (X_b), carbon conversion efficiency (η_{cc}), cold gas efficiency (η_g), and syngas yield (Y). Temperature, T_{FR}=940 ºC; steam-to-biomass ratio, S/B=0.6.

Submitted, accepted and published by:
Chemical Engineering Journal 405 (2021) 126679
https://doi.org/10.1016/j.cej.2020.126679

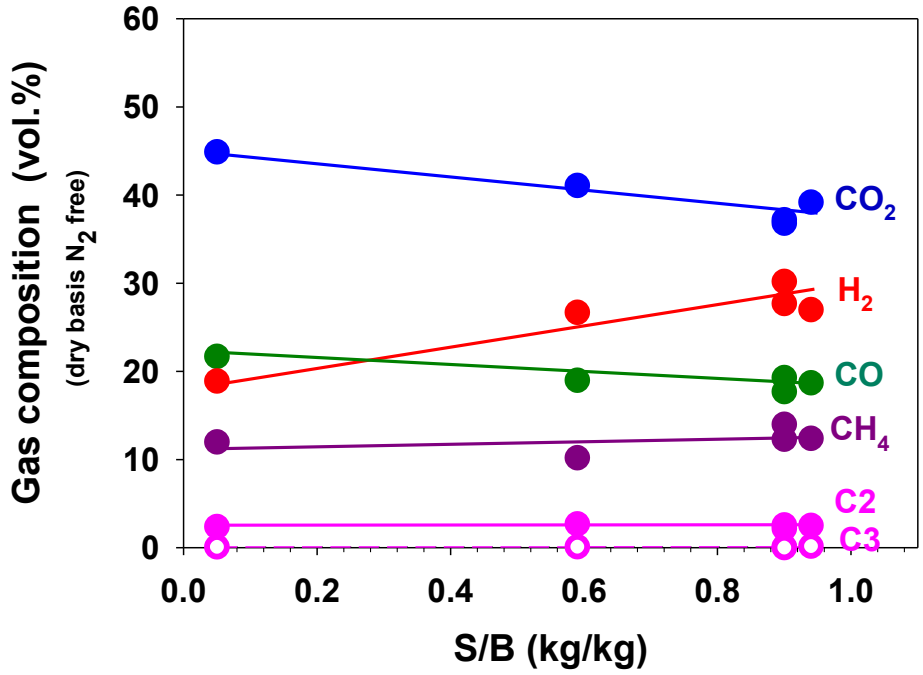

Figure 7. Effect of steam-to-biomass ratio, S/B, on the syngas composition. Temperature, T_{FR}=880 ºC; oxygen-to-biomass ratio, λ≈0.3.

Submitted, accepted and published by:
Chemical Engineering Journal 405 (2021) 126679
https://doi.org/10.1016/j.cej.2020.126679

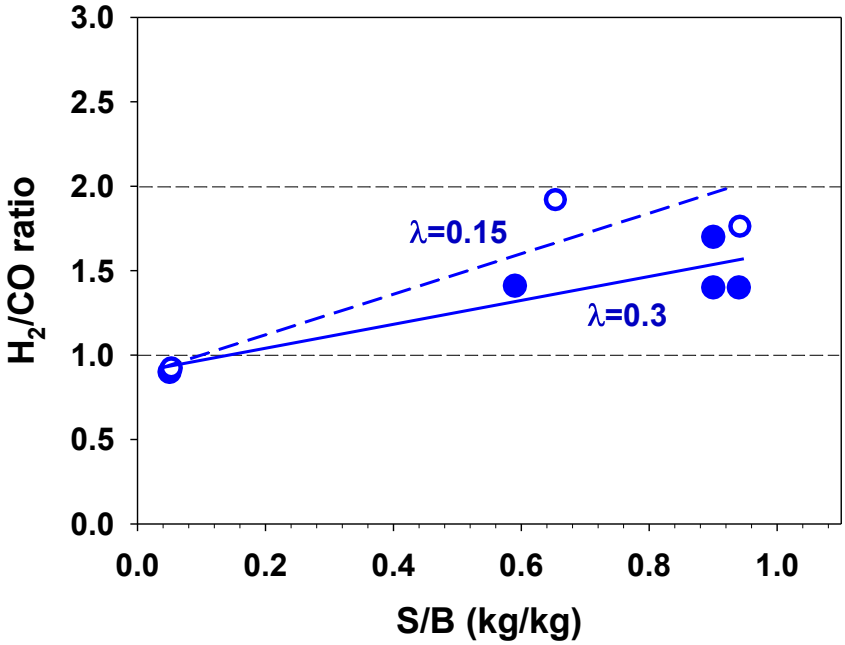

Figure 8. Effect of steam-to-biomass ratio, S/B, on the H_2/CO ratio. Temperature, T_{FR}=880 ºC; oxygen-to-biomass ratios, λ≈0.15 and 0.3.

Submitted, accepted and published by:
Chemical Engineering Journal 405 (2021) 126679
https://doi.org/10.1016/j.cej.2020.126679

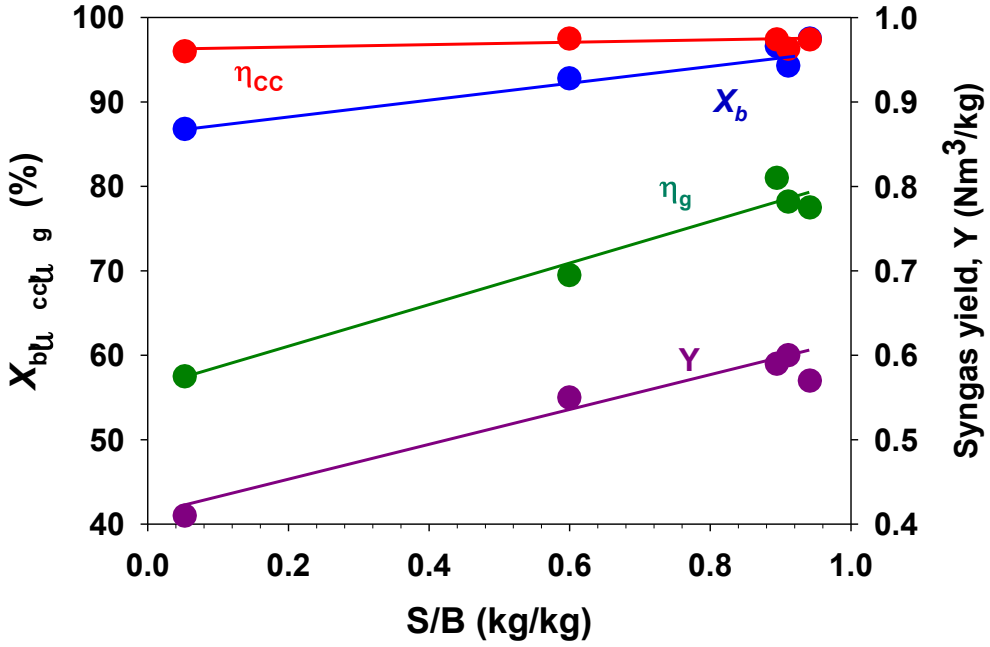

Figure 9. Effect of steam-to-biomass ratio, S/B, on the biomass conversion (X_b), carbon conversion efficiency (η_{cc}), cold gas efficiency (η_g), and syngas yield (Y). Temperature, T_{FR}=880 ºC; oxygen-to-biomass ratio, λ≈0.3.

Submitted, accepted and published by:
Chemical Engineering Journal 405 (2021) 126679
https://doi.org/10.1016/j.cej.2020.126679

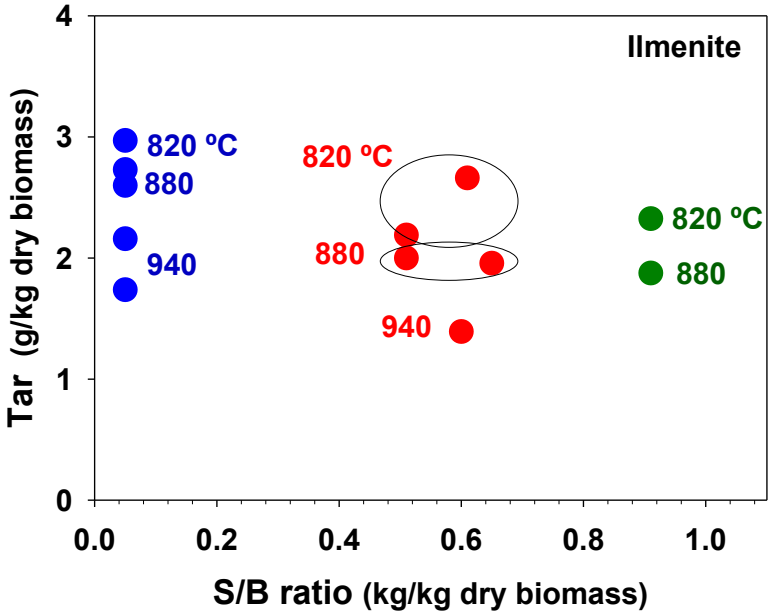

Figure 10. Tar generation during BCLG process using ilmenite as oxygen carrier.

Submitted, accepted and published by:
Chemical Engineering Journal 405 (2021) 126679
https://doi.org/10.1016/j.cej.2020.126679

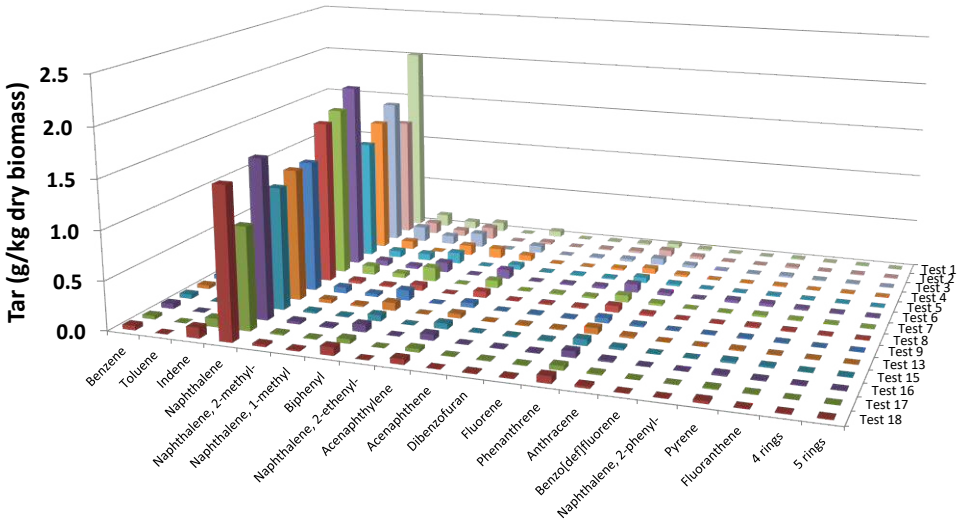

Figure 11. Tar generation during CLG process using ilmenite as oxygen carrier.

Submitted, accepted and published by:
Chemical Engineering Journal 405 (2021) 126679
https://doi.org/10.1016/j.cej.2020.126679

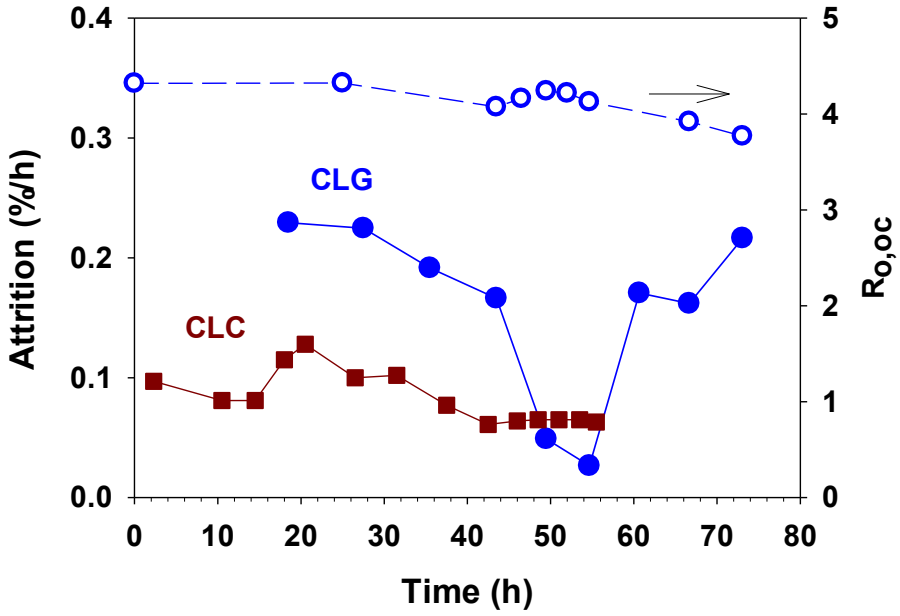

Figure 12. Comparison of the attrition rate of ilmenite operating under CLC and CLG conditions, and evolution of the oxygen transport capacity, $R_{o,oc}$.

Submitted, accepted and published by:
Chemical Engineering Journal 405 (2021) 126679
https://doi.org/10.1016/j.cej.2020.126679

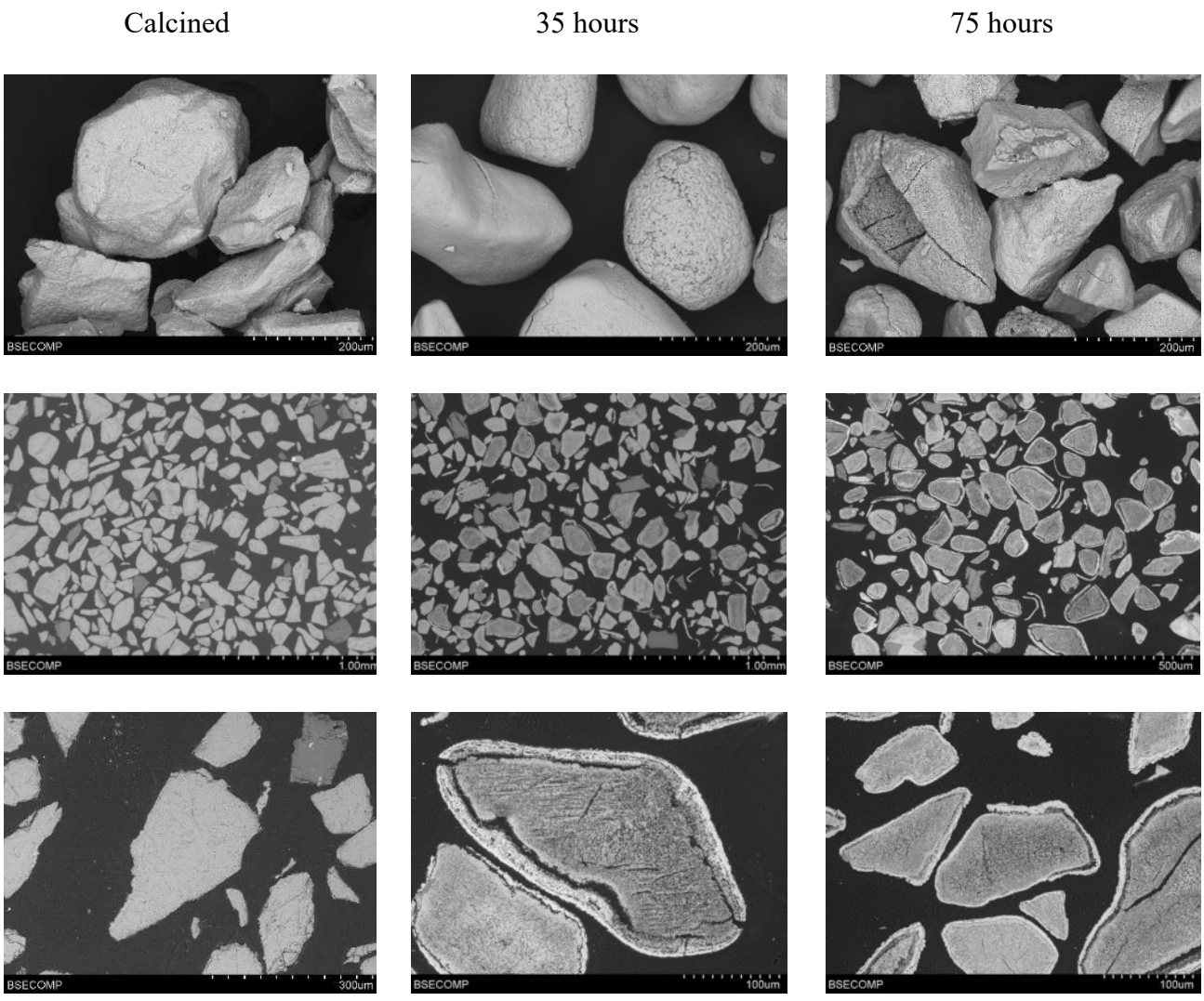

Figure 13. SEM images of the fresh and used ilmenite particles under BCLG conditions.

Submitted, accepted and published by:
Chemical Engineering Journal 405 (2021) 126679
https://doi.org/10.1016/j.cej.2020.126679

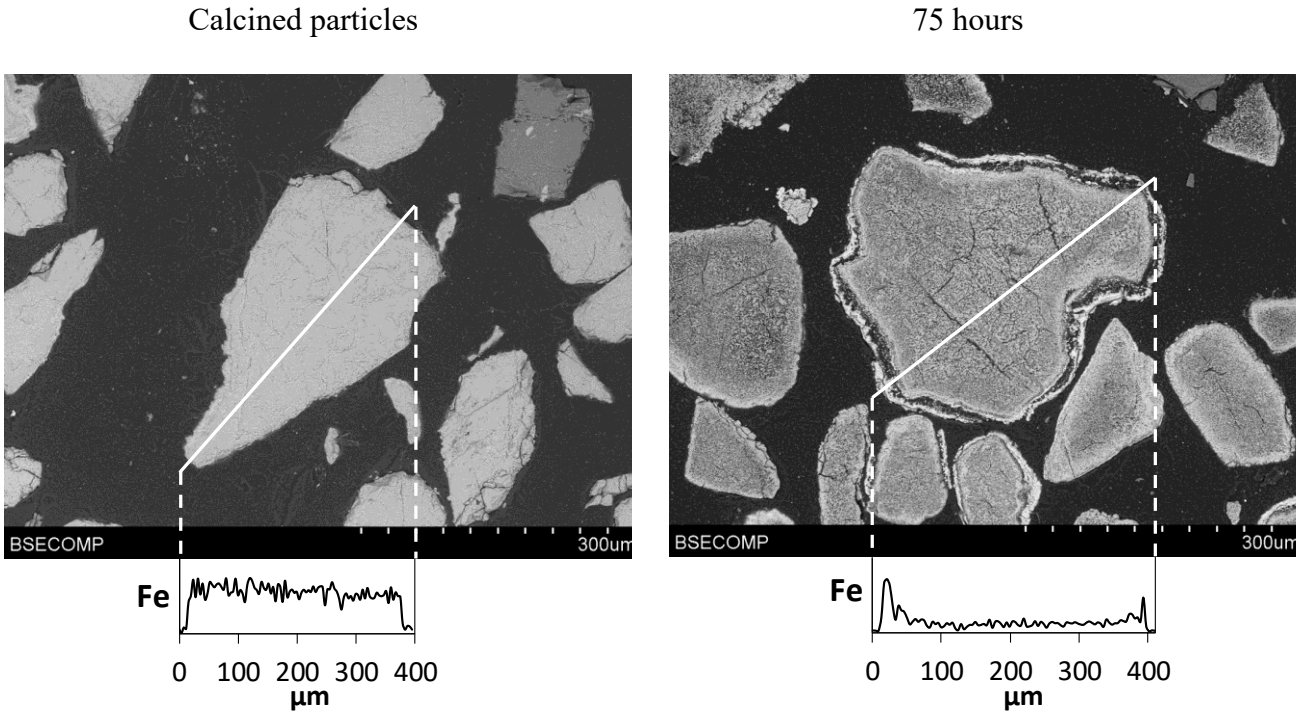

Figure 14. SEM-EDX images of the ilmenite particles under BCLG conditions.

Submitted, accepted and published by:
Chemical Engineering Journal 405 (2021) 126679
https://doi.org/10.1016/j.cej.2020.126679

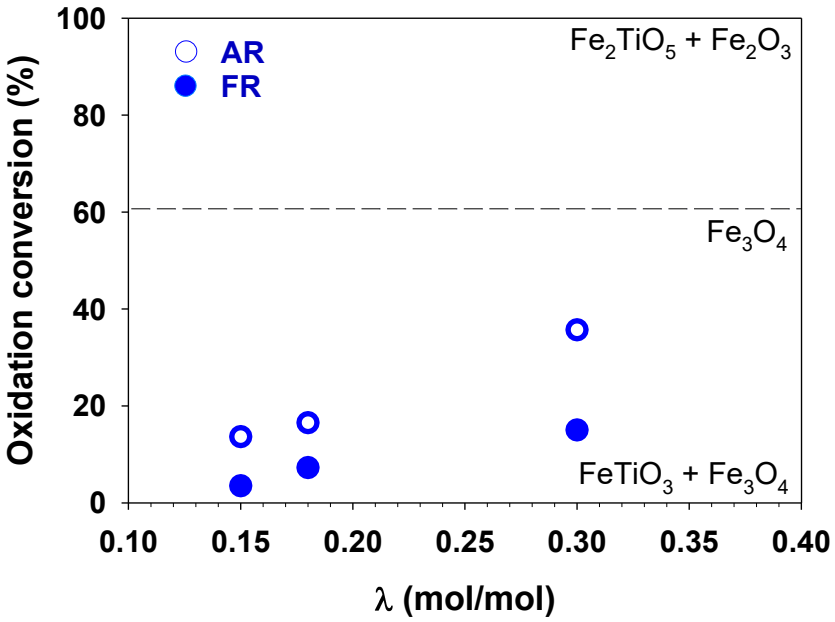

Figure 15. Oxidation degree of samples extracted from the fuel and air reactors as a function of the oxygen-to-biomass ratio, λ.